

## 671 **Supplementary methods and figures**

### 672 **1.1 Flow cytometric analysis**

673 GBM8401 and T98G cells were seeded in six-well plates ( $10^5$  cells/well) overnight and treated with CC12  
674 for 48 h. After treatment, cells were harvested, fixed, counted, and stained with different antibodies or dyes  
675 as previously described [1, 2]. Staining reagents are listed as follows: FITC-DEVD-FMK (cleaved  
676 caspase-3), FITC-IETD-FMK (cleaved caspase-8), FITC-VAD-FMK (cleaved caspase-9), Fas-PE,  
677 Fas-FITC, DIOC<sub>6</sub> (for the mitochondrial membrane potential), propidium iodide (PI), and FITC Annexin V  
678 Apoptosis Detection Kit (BD Bioscience, Franklin Lakes, NJ, USA). Fluorescence signals emitted from  
679 stained cells were determined by flow cytometry (NovoCyte, Agilent Technologies, Santa Clara, CA, USA)  
680 and quantified by FlowJo software (vers. 7.6.1; FlowJo LLC, Ashland, OR, USA).

### 681 **1.2 Invasion and migration (metastasis) analysis**

682 GBM8401 and T98G cells were seeded in 10-cm plates ( $10^6$  cells/plate) overnight and treated with CC12 for  
683 48 h. After treatment,  $10^5$  cells were harvested, counted, and seeded into transwells with 30% Matrigel  
684 (invasion) or without (migration). Cells were allowed to migrate or invade for 48 h, fixed with fixation  
685 buffer (methanol: acetic acid = 3: 1) and stained with 0.1% crystal violet for 15 min [3]. GBM8401 cells  
686 after small hairpin (sh)RNA-knockdown and overexpression were also used to performed the invasion  
687 experiment. Transwell membranes were then isolated for visualization with a Nikon ECLIPSE Ti-U  
688 microscope (Tokyo, Japan) and quantified by ImageJ software vers. 1.50 (National Institutes of Health  
689 (NIH), Bethesda, MD, USA).

### 690 **1.3 Western blot analysis**

691 GBM8401 and T98G cells were seeded in 10-cm plates ( $3 \times 10^6$  cells/plate) overnight and treated with CC12  
692 for 48 h. After treatment, cells were harvested, lysed with NP-40 buffer (containing a phosphatase and  
693 proteinase inhibitor cocktail), and quantified by the Bradford assay. Proteins were then separated by sodium  
694 dodecylsulfate (SDS)-polyacrylamide gel electrophoresis (PAGE) (8%~15%), transferred onto

695 polyvinylidene difluoride (PVDF) membranes, stained with the primary antibody, followed with the  
696 secondary antibody, visualized by a chemiluminescent horseradish peroxidase (HRP) substrate, and finally  
697 detected by UVP ChemiDoc-It™ (Analytik Jena, Jena, Germany) as previously described [4]. Primary and  
698 secondary antibodies are listed in Table 2.

#### 699 **1.4 Generation of lentiviral particles for knockdown and overexpression of LYN**

700 Three lentiviral transfer vectors, viz., pGFP-C-shLenti (TR30023) targeting different regions of LYN (Gene  
701 ID = 4067; TL320407A and TL320407B) and a non-effective 29-mer scrambled shRNA (pGFP-C-shLenti  
702 Vector; TR30021) were ordered from OriGene. Lentiviral particles were produced by transfecting HEK  
703 293T cells with a trans-packaging plasmid mix (shRNA vector, packaging plasmid: pCMV- $\Delta$ R8.91 and  
704 envelope plasmid: pMD.G, a VSV-G expressing plasmid) and TransIT®-LT1 Transfection Reagent (Mirus  
705 Bio LLC, Madison, WI, USA). HEK 293T cells were incubated for 18 h. The medium was changed and  
706 replaced with 10 mL bovine serum albumin (BSA)-containing medium (1% BSA) for 18 h. Media were  
707 harvested after incubation for 40 and 64 h. Lentivirus packages were stored at -80 °C for long-term storage.  
708 The human LYN open reading frame (NM\_001111097) was inserted into the pLenti-C-mGFP-P2A-Puro  
709 (PS100093) vector ordered from OriGene. Lentiviral particles were produced in HEK 293T cells by  
710 transfecting cells with the pLenti-C-mGFP LYN vector (SR175449) and trans-packaging plasmid mix  
711 (packaging plasmid: pCMV- $\Delta$ R8.91 and envelope plasmid: pMD.G, aVSV-G-expressing plasmid) and  
712 using the TransIT®-LT1 Transfection Reagent.

#### 713 **1.5 Knockdown and overexpression of LYN**

714 GBM8401 cells were virally transfected with pGFP-C-shLenti (scrambled)/pGFP-C-shLenti-LYN and  
715 pLenti-C-mGFP-P2A-Puro (MOCK)/pLenti-C-mGFP-P2A-Puro-LYN (overexpression). GBM8401 cells at  
716 50% confluence were incubated for 24 h in a 1:9 dilution of the virus package with 4  $\mu$ g/ml polybrene. After  
717 24 h of recovery in normal culture medium with no virus, cells were selected with 1  $\mu$ g/ml puromycin for 7  
718 days before being used in subsequent experiments.

## 719 **1.6 NF- $\kappa$ B transfection and *in vivo* reporter gene assay**

720 GBM8401 cells were transfected with pNF- $\kappa$ B-luc2, selected as a stable clone by 200  $\mu$ g/ml hygromycin B  
721 and named GBM8401/NF- $\kappa$ B-luc2 [5]. For animal experiments, the GBM8401/NF- $\kappa$ B-luc2 signal from  
722 mice brains was detected by the IVIS200 Imaging System after intraperitoneally injecting 150 mg/kg body  
723 weight D-luciferin. The signal intensity of NF- $\kappa$ B in mice brains was quantified through drawing regions of  
724 interest (ROIs) with Living Image software.

## 725 **1.7 Protein kinase array**

726 The human RTK Phosphorylation Array C1 was purchased from RayBio® (RayBiotech Life, Norcross, GA,  
727 USA). GBM8401 cells were treated with 0 and 20  $\mu$ M of CC12 for 48 h, and proteins were extracted to  
728 perform the experiment. Array membranes were incubated with 1 ml (250  $\mu$ g) of protein lysis of GBM8401  
729 cells overnight at 4 °C. After washing the membranes, they were incubated with biotin-conjugated  
730 antibodies (mouse Biotinylated Antibody Cocktail) overnight. Then, membranes were incubated with  
731 streptavidin-HRP for 2 h and a chemiluminescence reagent mix for 2 min. Immunoreactive dots on the  
732 membranes were detected by a chemiluminescent image system (ChemiDoc-It 515, UVP, Upland, CA,  
733 USA).

## 734 **1.8 GeneMANIA and GEPIA analysis**

735 The keywords of LYN, STAT3, MAPK1/2, and NF- $\kappa$ B were filled in the geneMANIA system for  
736 identifying the correlation of each other in Homo sapiens. We utilized RNA data sets from The Cancer  
737 Genome Atlas open-source collection, which can be accessed through the GEPIA website. GEPIA (Gene  
738 Expression Profiling Interactive Analysis) is an online resource for gene expression analysis and survival  
739 relation with specific gene. Here, we used input LYN, HGFR, TKY2 gene that we illustrated from CC12  
740 protein kinase array.

741

## 742 **1.9 Preparation of $^{68}\text{Ga}$ radioisotope labeled CC-12.**

743 To prepare  $^{68}\text{Ga}$  labeled CC-12, first 1 mL of  $^{68}\text{Ga}$  is added to CC-12. The mixture is then agitated on a 300  
744 rpm shaker at 37 °C for 10-30 minutes to produce  $^{68}\text{Ga}$ -CC-12. To purify the mixture, a centrifuge is used at  
745 14,000 rpm for 10 minutes with a 10k centrifuge tube (Sartorius Vivaspin®, Göttingen, Germany). The  
746 supernatant liquid is removed, and the particles are suspended in normal saline and repeated once. Finally,  
747 the radiolabeling yield and radiochemical purity are checked using an instant thin layer chromatography  
748 system (AR-2000 radio-TLC Imaging Scanner, Bioscan Inc., Poway, CA, USA).

### 749 **1.10 *In vivo* Nano-SPECT/CT scan**

751 For the investigation of *in vivo* biodistribution of  $^{68}\text{Ga}$ -CC-12, the signal of it (Activity equivalent to 37  
752 MBq) in mice were obtained by using Positron Emission Tomography - Computed Tomography (PET/CT).  
753 The  $^{68}\text{Ga}$ -CC-12 particles in 100  $\mu\text{L}$  of normal saline was injected through intravenous injection. The signal  
754 of  $^{68}\text{Ga}$ -CC-12 in the mouse brain was assessed immediately using a NanoScan PET/CT scanner system  
755 (Mediso, Arlington, VA, USA) following injection. Following the capture of the PET images, CT images  
756 were acquired (X-ray source: 70 kV, 1 mA; 256 projections) at the same position. The images were fusion  
757 by using InVivoScope® software. To ensure proper imaging, the mice were anesthetized with inhalation of  
758 isoflurane (3-4%) during scanning.

### 759 **1.11 Biodistribution of $^{68}\text{Ga}$ -CC-12**

761 The biodistribution study of  $^{68}\text{Ga}$ -free or  $^{68}\text{Ga}$ -CC-12 in mice was conducted on normal mice, mice with  
762 GBM8401 tumor (150~200  $\text{mm}^3$ ), 6Gy RT whole brain exposure model (n=3), respectively. Mice were  
763 anesthetized with isoflurane and injected with  $^{68}\text{Ga}$ -CC-12 (3.7 MBq) through the intra-carotid artery. After  
764 10 min, 1 hr or 3 hr min injection, mice were sacrificed by  $\text{CO}_2$ . The organs were excised, weighed, and  
765 assayed for radioactivity by gamma counter (1470Wizard, PerkinElmer, Waltham, MA, USA). The tissue  
766 activity was displayed as percentage injected dose per gram of tissue (%ID/g).

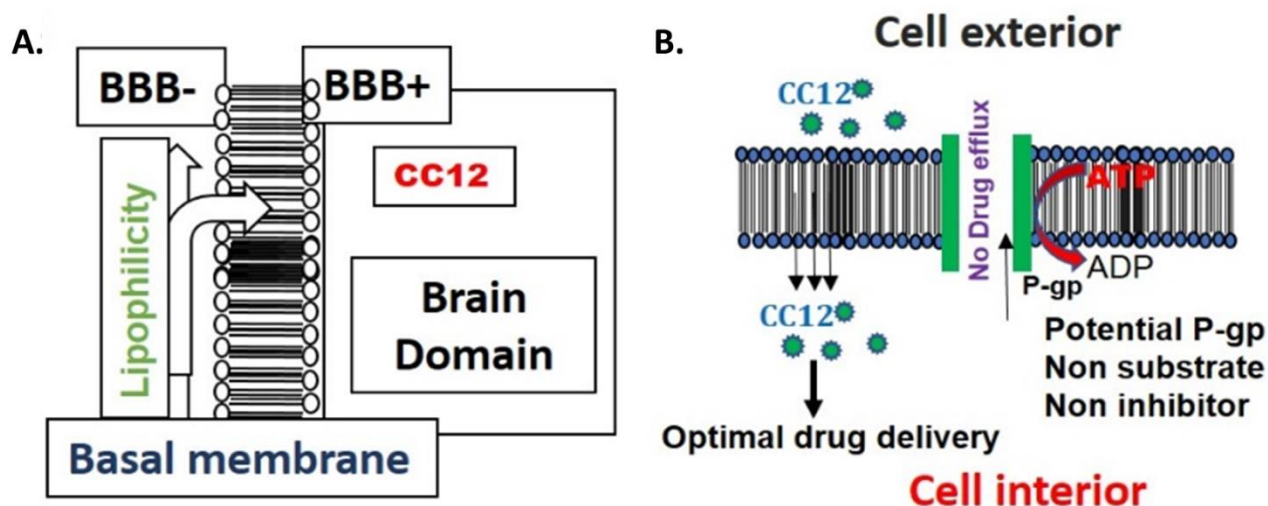
767 **1.12 Hematoxylin and eosin (H&E) staining and immunohistochemical (IHC) staining**

768 Mice tumors were isolated for staining on day 21. The staining procedure was described in previous work  
769 [6]. Images were scanned with a TissueFAXS Tissue-Gnostics Axio Observer Z1 microscope  
770 (TissueGnostics) and quantified by the ImageJ IHC tool box developed by the NIH [7].

771 **1.13 BBB permeation algorithm**

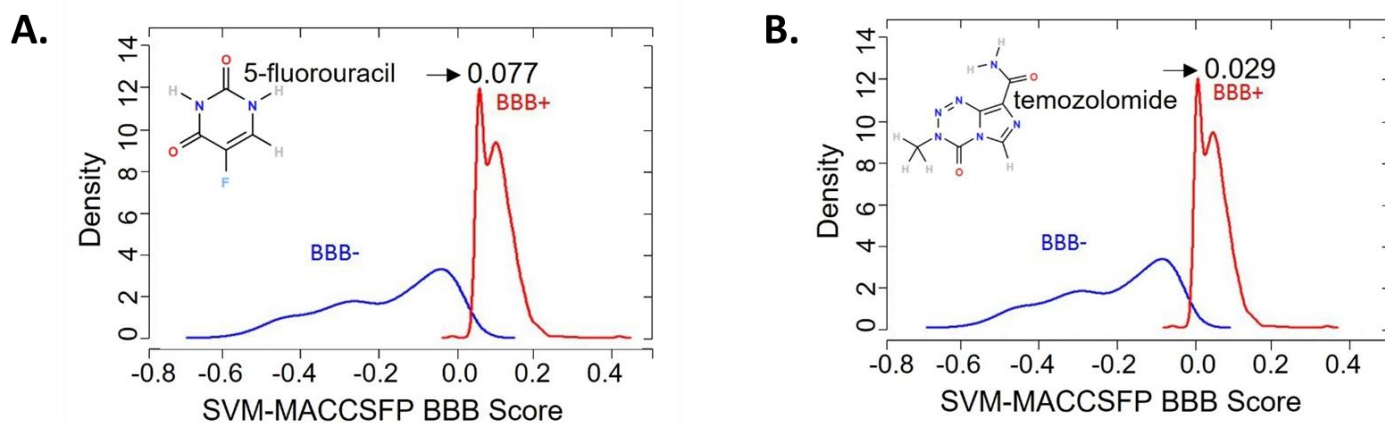
772 The BBB permeability graph was built using the ALzPlatform, a BBB permeation algorithm that applies  
773 support vector machine (SVM) and LiCABEDS algorithms to simulate drug density that pass the BBB. The  
774 algorithm used the physicochemical properties and structural coordinate of the drugs to simulate the peak  
775 density corresponding to the scores of the drugs BBB permeability.

776



778

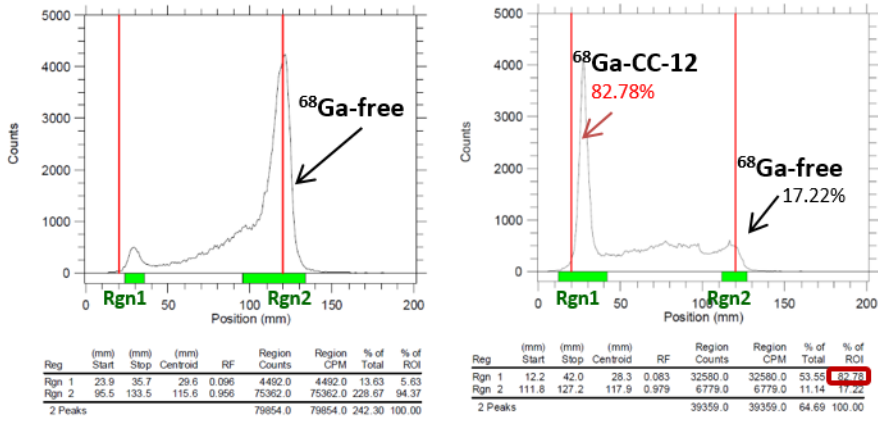
779 **Supplementary figure 1.** Figure demonstrated non-substrability and non-inhibitor tendencies towards P-gp  
780 of CC12.



781

782 **Supplementary figure 2.** In silico BBB permeability curve of (A) 5-FU and (B) TMZ based on support  
783 vector machine (SVM) and LiCABEDS algorithms is displayed.

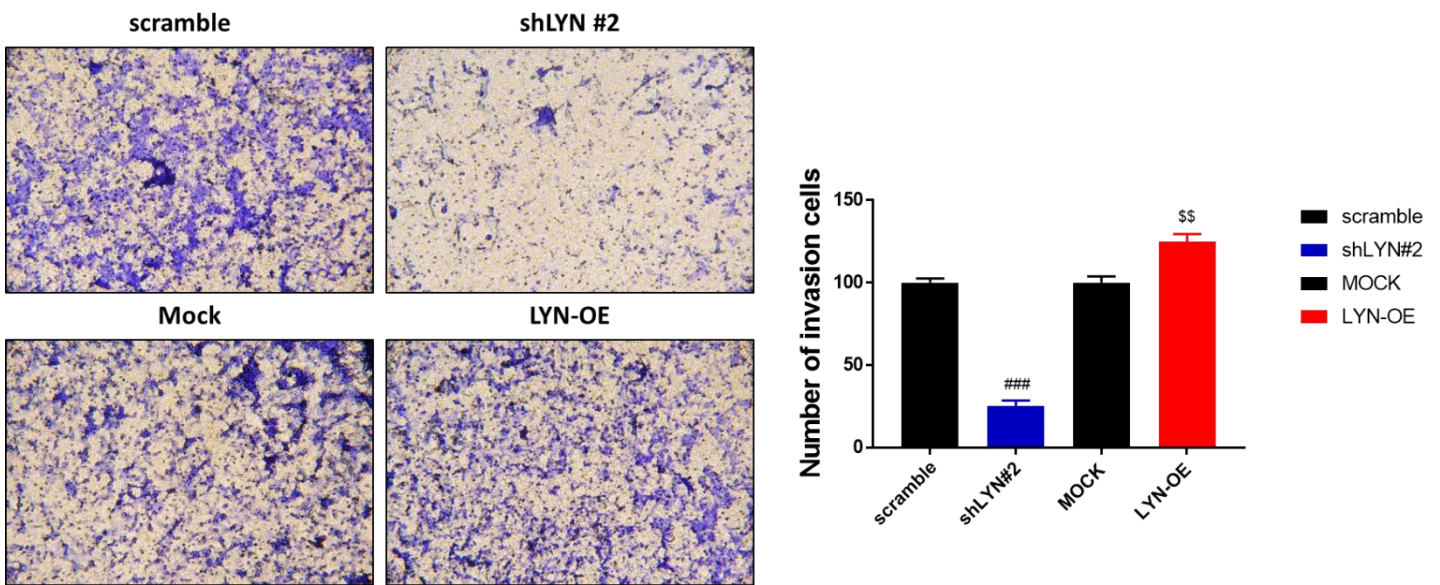
784



785

786

**Supplementary figure 3.** The  $^{68}\text{Ga}$  labeling efficacy on CC12 is displayed.



787

788

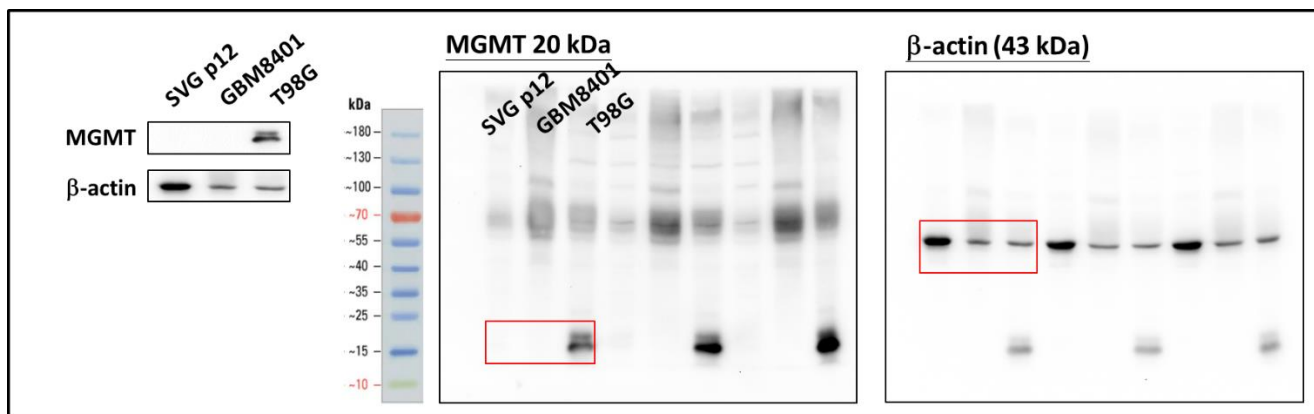
**Supplementary figure 4.** Invasion results in LYN knockdown and overexpression GBM8401 cells.

789

790

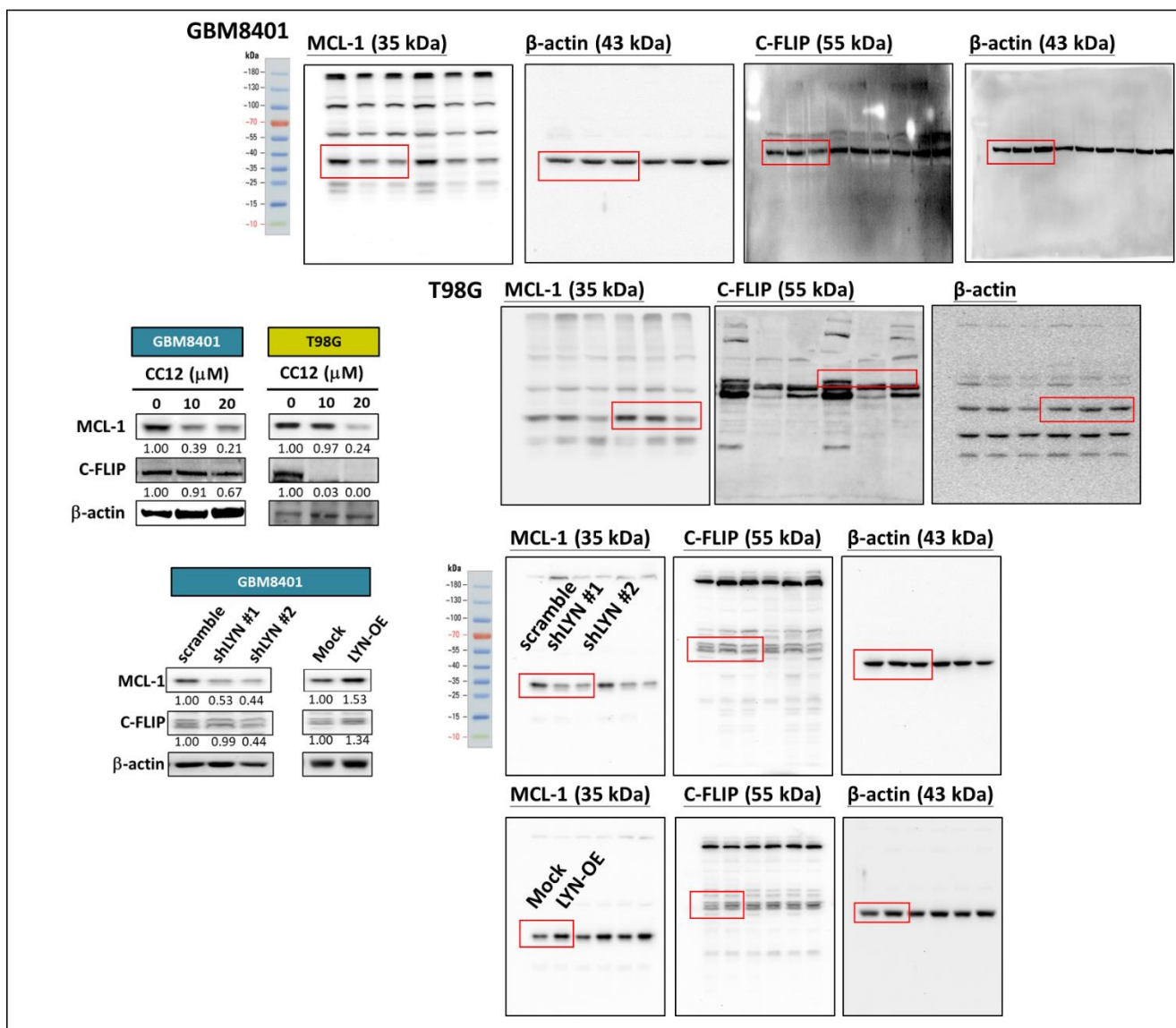
791 **Supported data**

792 3.1 Full blot images of Figure 2A



793

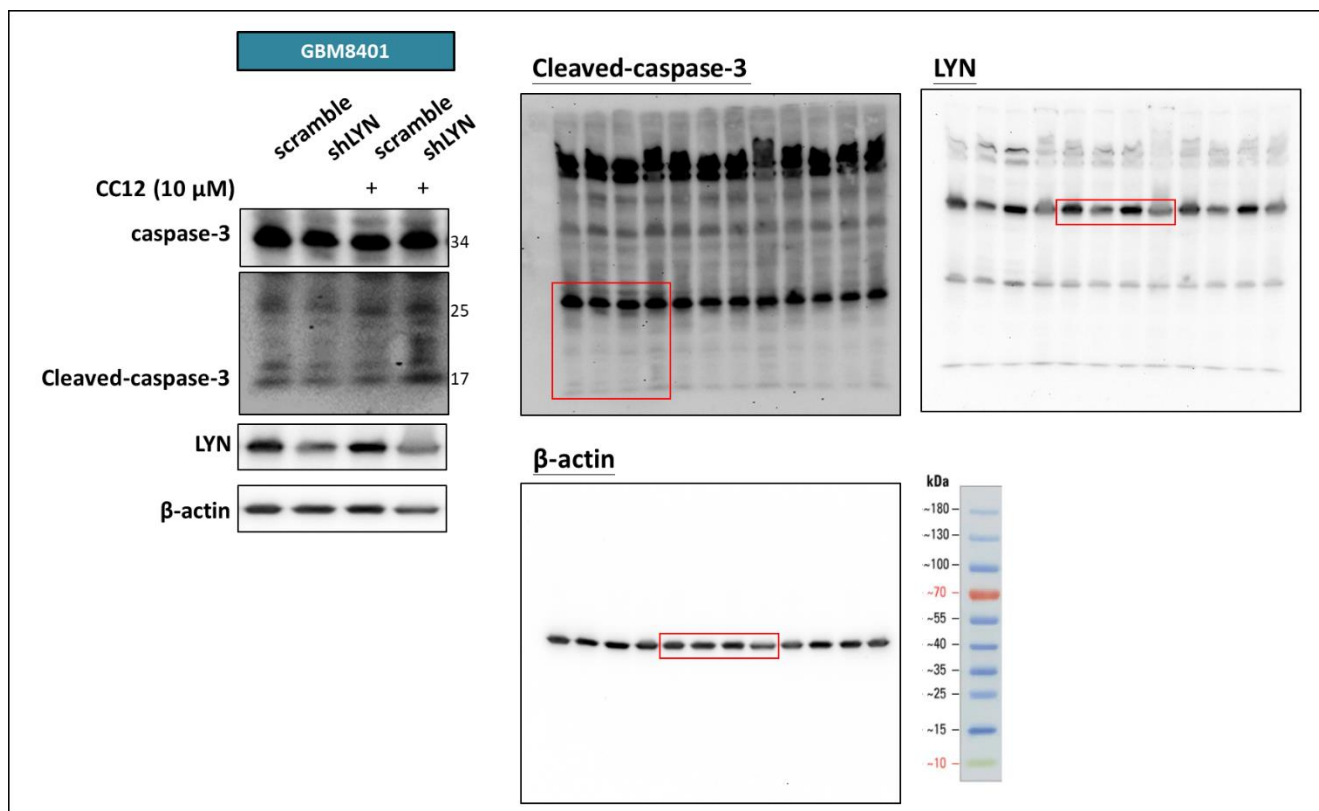
794 3.2 Full blot images of Figure 3D



795

796

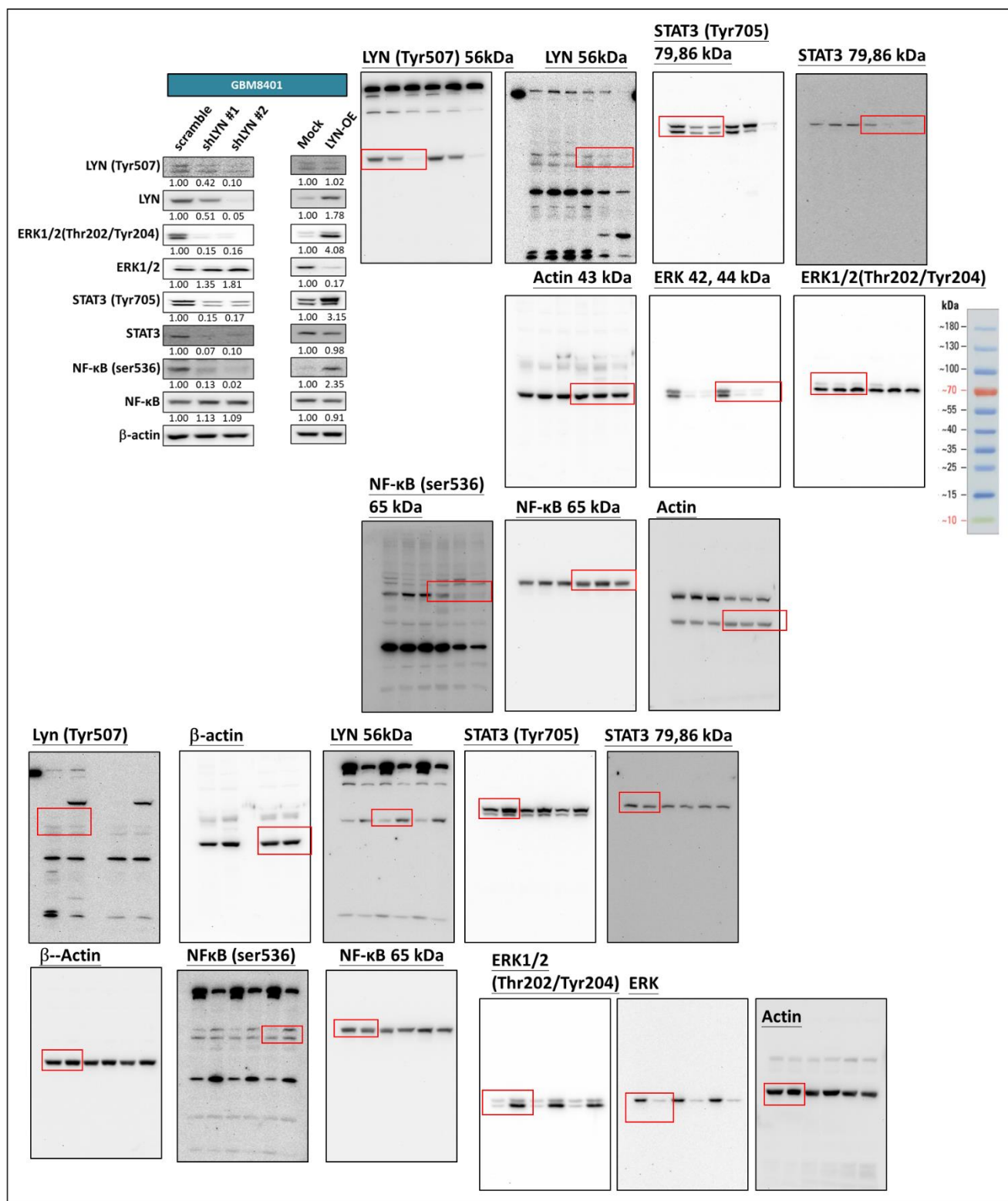




798

799

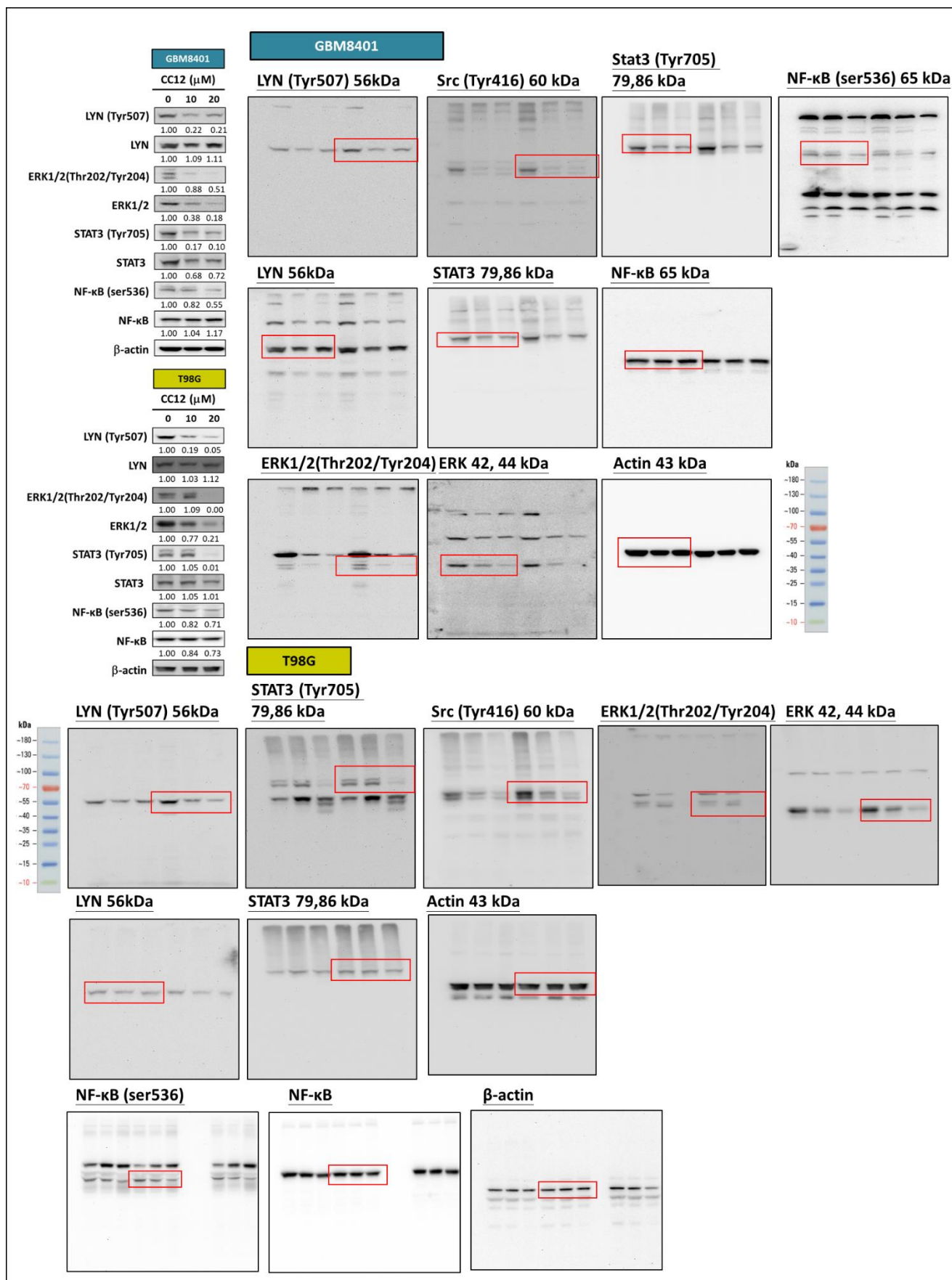
800

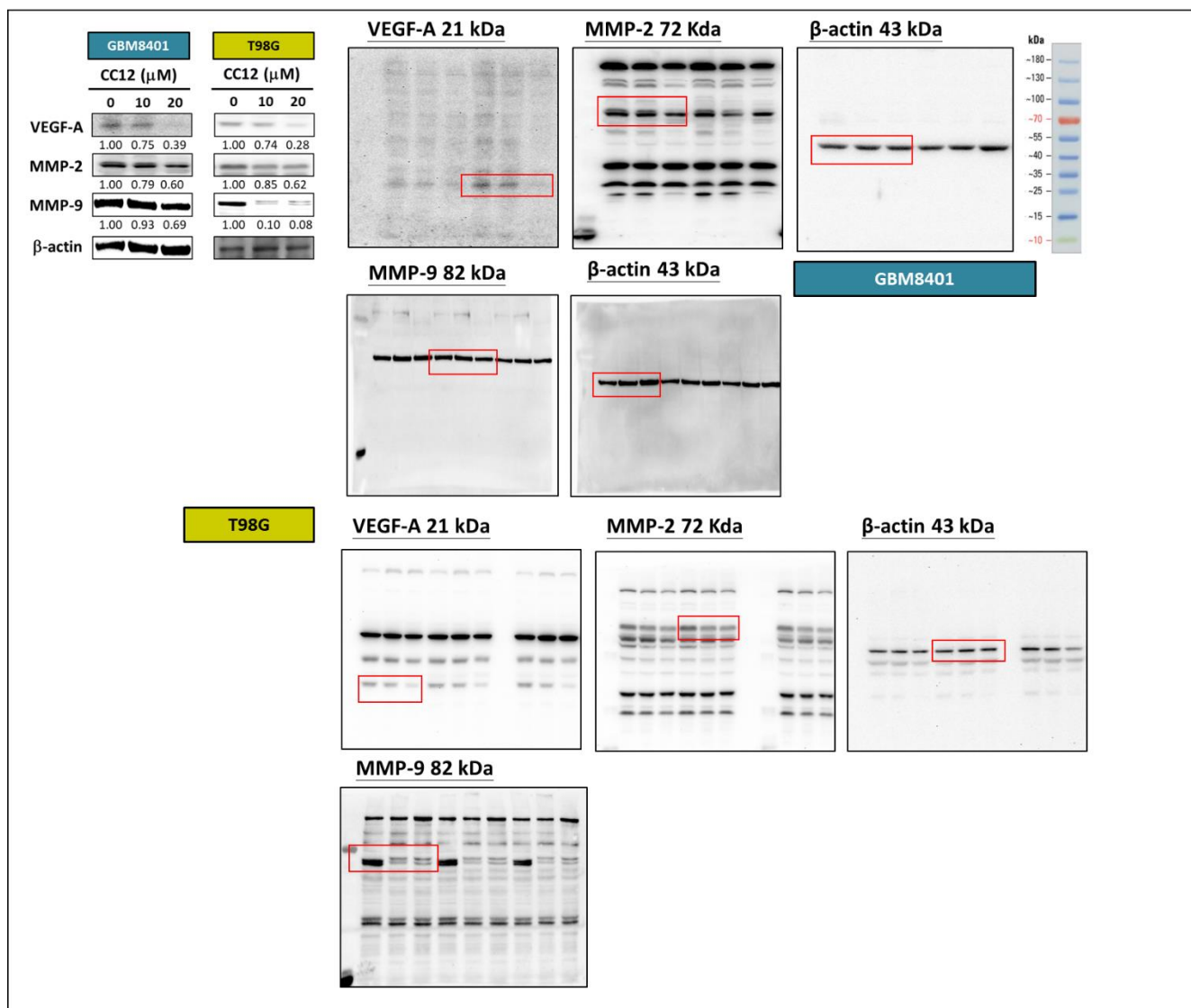


802

803

804

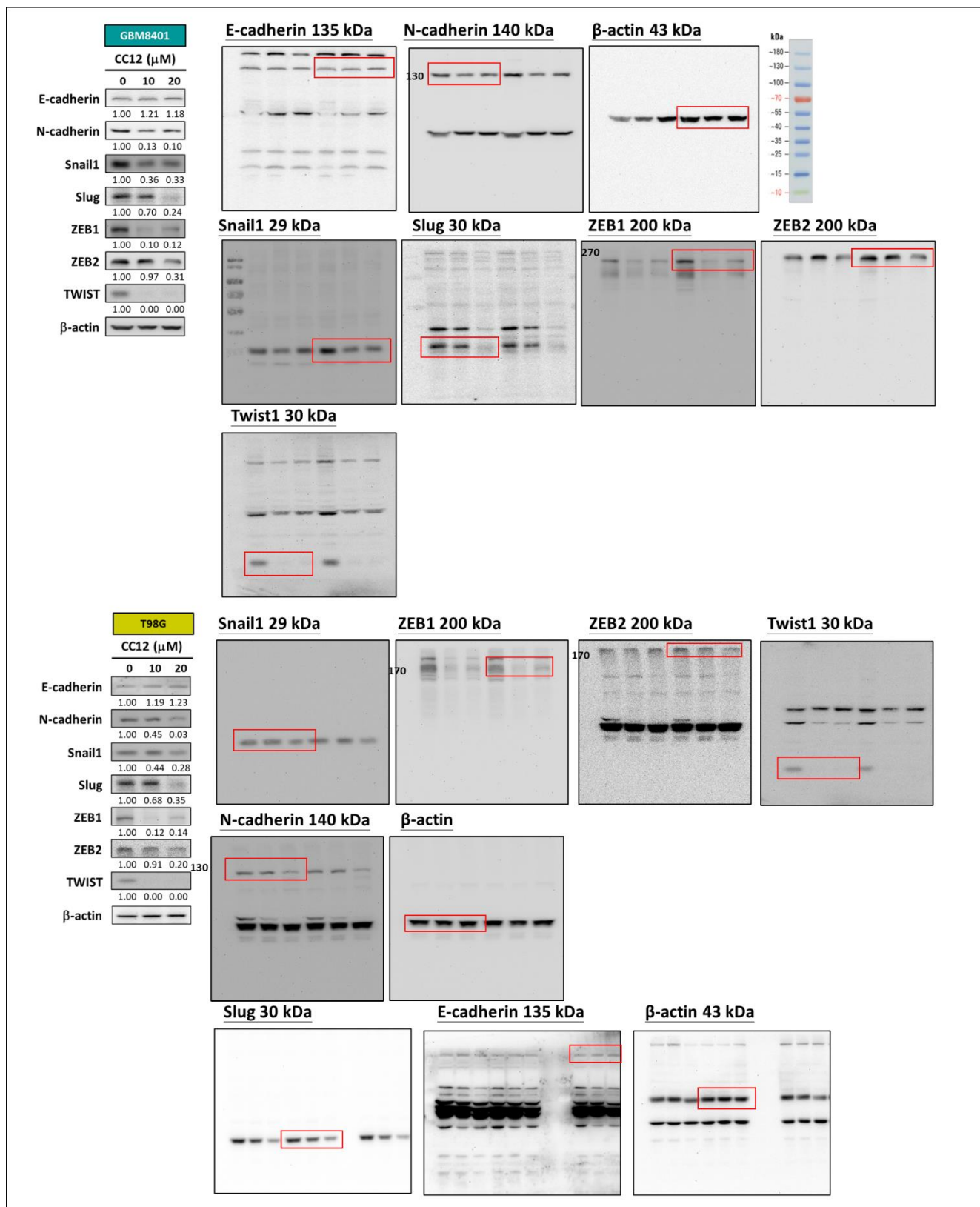




808

809

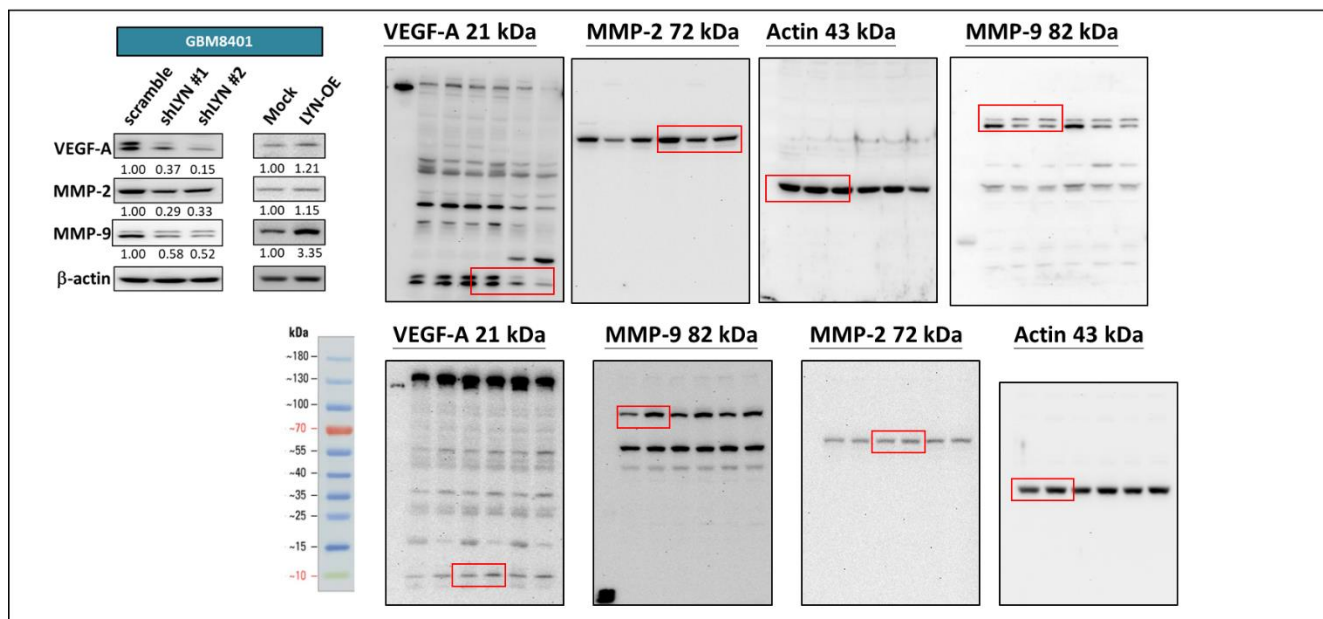
810

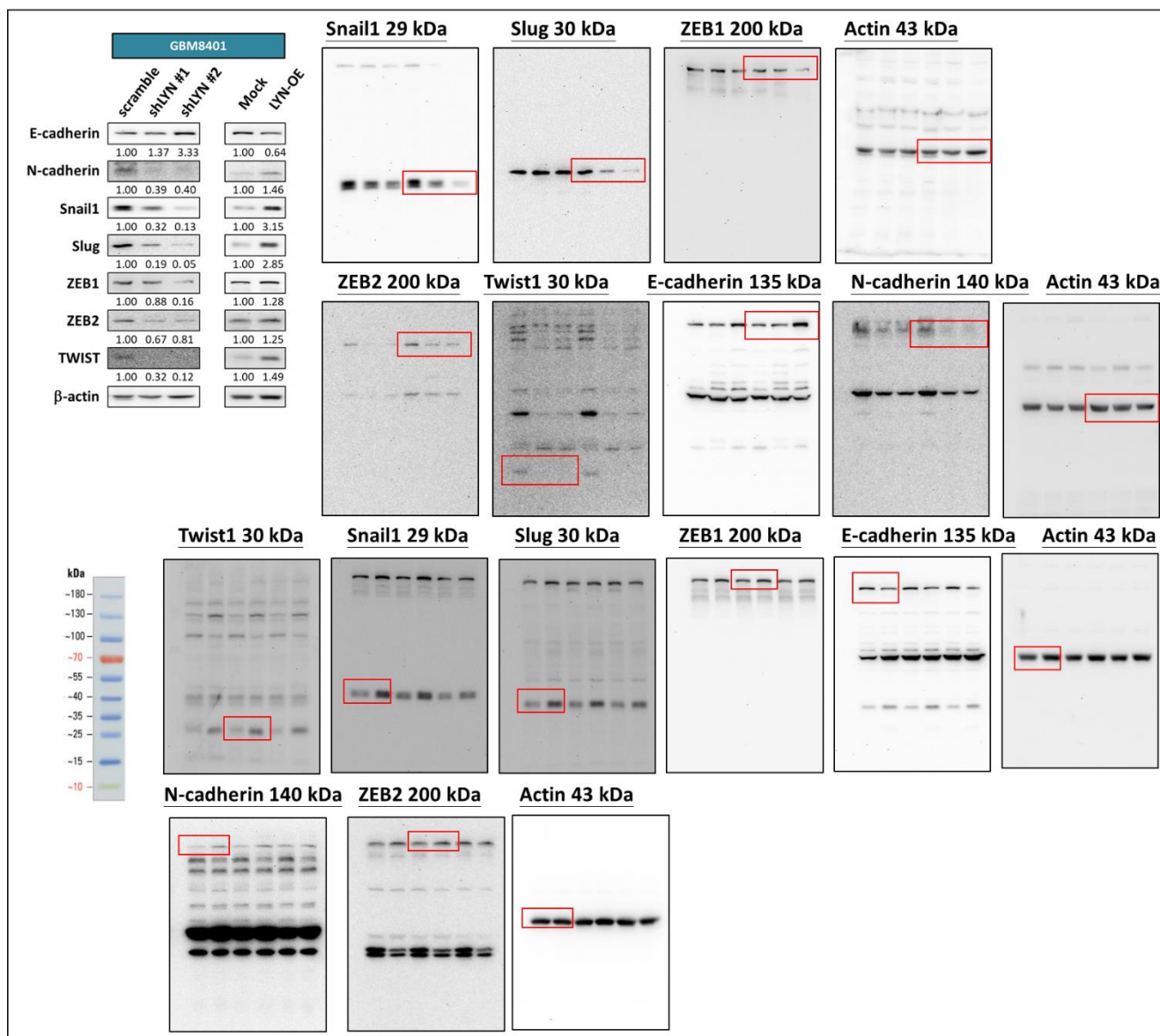


812

813

814





818

819 **References**

820 1. Chiang IT, Chen WT, Tseng CW, Chen YC, Kuo YC, Chen BJ, et al. Hyperforin Inhibits Cell Growth  
821 by Inducing Intrinsic and Extrinsic Apoptotic Pathways in Hepatocellular Carcinoma Cells. *Anticancer*  
822 *Res.* 2017; 37: 161-7.

823 2. Chiang CH, Chung JG, Hsu FT. Regorefenib induces extrinsic/intrinsic apoptosis and inhibits  
824 MAPK/NF-κB-modulated tumor progression in bladder cancer in vitro and in vivo. *Environ Toxicol.*  
825 2019; 34: 679-88.

826 3. Yueh PF, Lee YH, Fu CY, Tung CB, Hsu FT, Lan KL. Magnolol Induces the Extrinsic/Intrinsic  
827 Apoptosis Pathways and Inhibits STAT3 Signaling-Mediated Invasion of Glioblastoma Cells. *Life*  
828 (Basel). 2021; 11.

- 829 4. Hsu FT, Chiang IT, Wang W-S. Induction of apoptosis through extrinsic/intrinsic pathways and  
830 suppression of ERK/NF- $\kappa$ B signalling participate in anti-glioblastoma of imipramine. *J Cell Mol Med.*  
831 2020; 24: 3982-4000.
- 832 5. Hsu FT, Chiang IT, Kuo YC, Hsia TC, Lin CC, Liu YC, et al. Amentoflavone Effectively Blocked the  
833 Tumor Progression of Glioblastoma via Suppression of ERK/NF-  $\kappa$  B Signaling Pathway. *Am J Chin*  
834 *Med.* 2019; 47: 913-31.
- 835 6. Hsu FT, Liu HS, Ali AAA, Tsai PH, Kao YC, Lu CF, et al. Assessing the selective therapeutic efficacy  
836 of superparamagnetic erlotinib nanoparticles in lung cancer by using quantitative magnetic resonance  
837 imaging and a nuclear factor kappa-B reporter gene system. *Nanomedicine.* 2018; 14: 1019-31.
- 838 7. Huang YP, Ma YS, Kuo CL, Liao CL, Chen PY, Peng SF, et al. Demethoxycurcumin Suppresses  
839 Human Brain Glioblastoma Multiforme GBM 8401 Cell Xenograft Tumor in Nude Mice In Vivo. *Int J*  
840 *Mol Sci.* 2021; 22.

841

842

843